

Resonance-Induced Delocalization of Electrons in GaAs-AlAs Superlattices

H. Schneider,^(a) H. T. Grahn, K. v. Klitzing, and K. Ploog

Max-Planck-Institut für Festkörperforschung, Heisenbergstrasse 1, D-7000 Stuttgart 80, Federal Republic of Germany

(Received 26 January 1990)

We report on novel interaction phenomena between different Stark ladders in a strongly coupled GaAs-AlAs superlattice. We observe an anticrossing behavior between certain exciton states if the electric field perpendicular to the layers of the superlattice is such that the energy spacing between the lowest two conduction subbands is an integer multiple of the Stark-ladder spacing. This anticrossing is accompanied by a spatial delocalization of the electron states and can therefore be resolved by photo-current spectroscopy. Our experimental results are confirmed by a numerical calculation of the field dependence of the conduction subband energies.

PACS numbers: 78.65.Fa, 73.20.Dx, 73.20.Jc, 78.20.Jq

Semiconductor superlattices (SLs) provide the unique possibility to generate a synthetic band structure that can be tailored in a wide range by varying the layer thicknesses of their constituents. This degree of freedom has recently been used to demonstrate Stark ladders and electric-field-induced localization of extended miniband states,¹⁻³ effects predicted 30 years ago by Wannier⁴ for the case of bulk crystals. Because of the correspondence between a miniband of a SL and a band of a bulk crystal, SLs are important model systems in order to obtain a better understanding of crystal properties. The possibility to observe Stark ladders in a bulk crystal has been a subject of controversial discussion in the literature.⁵ The complication arises from the occurrence of band mixing at high electric fields, a topic which was first investigated by Zener.⁶

In this Letter we report on a novel high-field superlattice effect which is observed in the GaAs-AlAs system. Our spectroscopic results show that large electric fields lead, in addition to the usually observed localization, also to delocalization effects if the system contains several Stark ladders. This delocalization is caused by the mixing of quantum states belonging to different Stark ladders. These mixing effects are observed between states centered not only in adjacent wells but also in nonadjacent wells, resulting in a delocalization over more than two SL periods. This interpretation is confirmed by numerical calculations.

The band structure of an ideal SL with period d at zero electric field F consists of minibands of delocalized states. Considering a single miniband of width 2Δ , the states become localized if $F > 0$ (Wannier-Stark localization). The resulting localization length is approximately $2\Delta/eFd$ SL periods.¹ The energy spectrum splits up into an infinite set of equidistant energy states (Stark ladder) separated by eFd . For $eFd > 2\Delta$, each state is almost completely localized within one SL period and behaves like a subband of an isolated quantum well. Analytic expressions for the field-dependent occupation probabilities in the individual wells are given in Ref. 1.

The situation becomes more complicated for the case

of several minibands since, at large enough electric fields, the resulting Stark-ladder states interact with each other. Figures 1(a) and 1(b) illustrate two special situations where the lowest subband mixes with the second subband centered in the neighboring [Fig. 1(a)] and

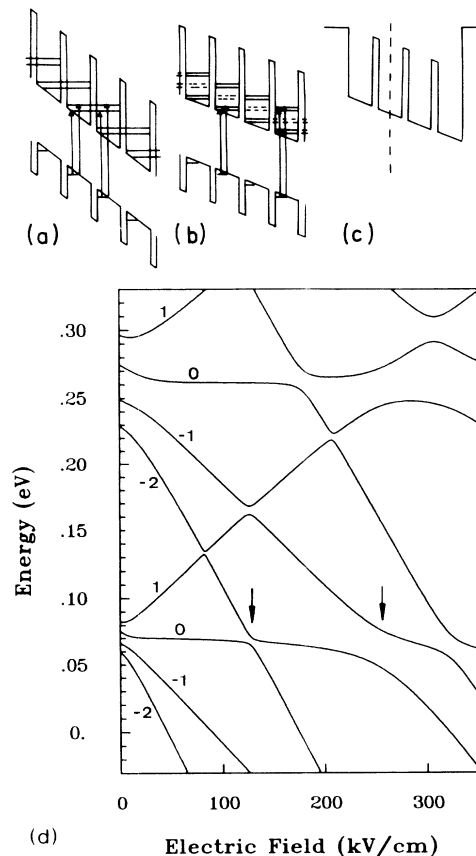


FIG. 1. Schematics of the transitions close to the (a) $m=1$ and (b) $m=2$ resonances. (c) Potential distribution at finite field of a system of four 7-nm GaAs wells separated by three 0.9-nm AlAs barriers. The dashed line indicates the spatial origin. (d) Calculated quantum energies vs electric field of the system of (c).

next-neighboring [Fig. 1(b)] wells. Figure 1(d) shows the quantum energies of the conduction band of a SL in an electric field, as obtained from a numerical solution of the Schrödinger equation in the two-band approximation^{7,8} using the band parameters of Ref. 9. As indicated in Fig. 1(c), the SL is approximated by a system of four coupled wells separated by three barriers. At $F=0$ there are two groups of four states each [Fig. 1(d)]. Each group corresponds to a discrete analog¹⁰ of a miniband in our four-well model. With increasing F these states depend approximately linearly on F with the slope given by $neFd$ ($n = -2, -1, 0, 1$). In this linear regime the corresponding wave functions are found to be almost completely localized within one well of the SL⁸ and one therefore obtains a well-defined subband spacing E_{21} between the two lowest subbands of each quantum well. The important feature now consists in the mixing between states which are localized in different, *not necessarily adjacent*, wells. In our calculation, the mixing manifests itself by an anticrossing behavior and by a delocalization of the participating wave functions into quantum states which are essentially linear combinations of the contributing localized states. The arrows at 260 and 130 kV/cm indicate the situations sketched in Figs. 1(a) and 1(b), respectively, which are characterized by the conditions $eFd = E_{21}$ and $2eFd = E_{21}$.

The generalization of these features to the case of an infinite SL is as follows. At low but finite electric fields, Wannier-Stark localization takes place, but now with an arbitrary integer n . The anticrossings arising between states deduced from the first and second minibands obey the resonance condition $meFd = E_{21}$, with m an integer (see also Ref. 5). This leads to an infinite number of anticrossings which accumulate at $F=0$. However, the energy repulsion decreases drastically with increasing m so that only a finite number of anticrossings can be resolved.

In our calculation, the quantum-confined Stark effect¹¹ (QCSE) of the individual wells produces field-dependent energy shifts. The largest shifts are achieved at high fields, e.g., 6 meV at 260 kV/cm for the lowest conduction subband. For excitonic transitions, the QCSE of the valence subbands (13 meV at 260 kV/cm for the first heavy-hole subband) induces an additional redshift. Since these values are negligible compared to the subband spacing E_{21} , a pattern similar to the one in Fig. 1(d) should be expected from a spectroscopic investigation of such a SL in an electric field.

In order to demonstrate these anticrossings experimentally, we have prepared a 60-period SL with 7-nm GaAs wells and 0.9-nm AlAs barriers. The SL is sandwiched between layers of 30 nm GaAs followed by 500-nm-wide $\text{Al}_{0.5}\text{Ga}_{0.5}\text{As}$ window layers. The $\text{Al}_{0.5}\text{Ga}_{0.5}\text{As}$ layers are n doped on the substrate side and p doped on the top side, respectively, both to about $5 \times 10^{17} \text{ cm}^{-3}$. The structure was grown by molecular beam epitaxy on a (100)-oriented n^+ substrate and processed into mesas of

450 μm diameter with Ohmic contacts of CrAu on the top and AuGeNi on the substrate side. Our photocurrent spectra were detected by a lock-in amplifier and corrected for the spectral dependence of the illumination system consisting of a halogen lamp and a double monochromator. The current-voltage (I - V) curves were detected by a HP4140B pA meter.

A series of photocurrent spectra are shown in Fig. 2. Flat-band condition ($F=0$) is at a bias of +1.48 V, the plus sign denoting forward direction. A change in bias of 1 V corresponds to a change in F of approximately 19 kV/cm. The signal increase between -15 and -17 V is due to avalanche multiplication. The region between 1.4 and -5 V shows the well-known¹⁻³ scenario of the blue-shift of the main absorption edge and Stark-ladder formation. The anticrossing associated with the $m=1$ resonance discussed above gives rise to pronounced structures around -14 V.

Before discussing the anticrossing in more detail it is important to distinguish this effect from the splitting of photoluminescence lines occurring in weakly coupled SLs.¹² In those systems, the transport probability is strongly enhanced if different subbands of adjacent wells are in resonance.^{8,13,14} This effect can lead to electric-field domains giving rise to additional spectroscopic lines¹² due to the Stark effect. For increasing electric field, those new lines appear at *lower* energies than the original lines. This is in contrast to the present situation where, for the transitions close to the SL band gap, the new lines appear at *higher* energies (see also Fig. 3).

We use in the following the notation $nCi-Hj$ and $nCi-Lj$ for the transition between the i th electron Ci and the j th heavy-hole Hj (light-hole Lj) subband with a spatial separation of n SL periods. For $n \neq 0$, this notation applies to the situation when the electron and hole wave functions exhibit small, spatially direct contribu-

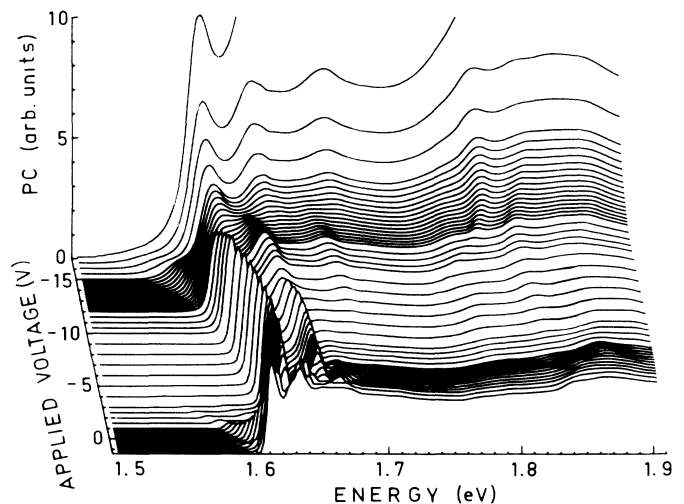


FIG. 2. Photocurrent vs energy at 5 K for different bias voltages from +1.4 to -17 V (quasi-3D representation).

tions but are mainly localized in different wells. At resonance, however, the spatially direct and indirect contributions to the electron wave functions under consideration have about the same amplitudes. This leads to the appearance of two, resonantly split excitonic transitions with an oscillator strength of half of the spatially direct, off-resonance transition.

The bias dependence of the peak energies of the photo-

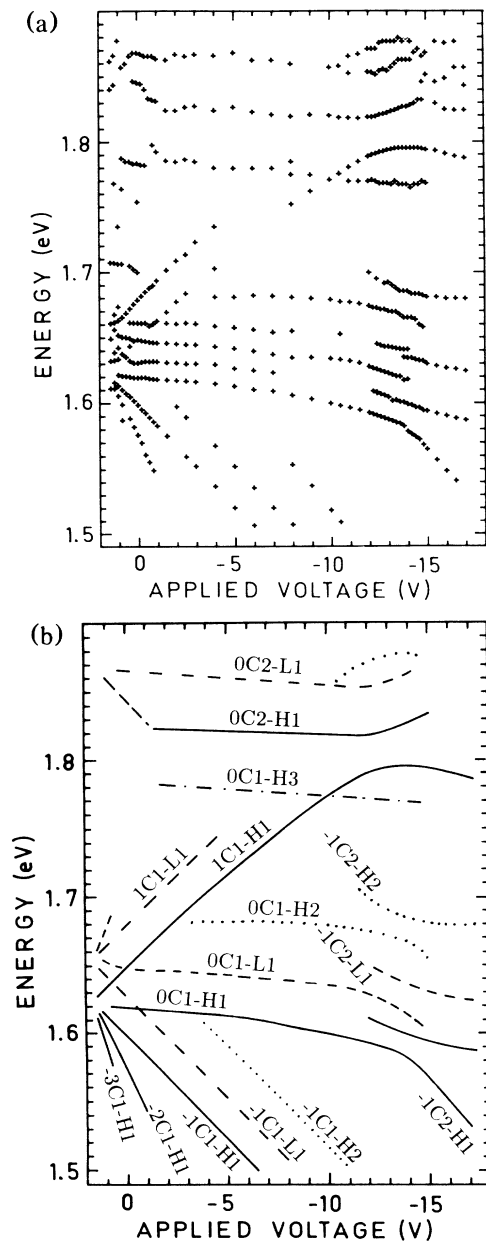


FIG. 3. (a) Peak energies of the spectra in Fig. 2 vs applied voltage. (b) Assignment of these peak energies to excitonic transitions. The lines refer to excitonic transitions due to the first heavy-hole (solid lines), first light-hole (dashed), second heavy-hole (dotted), and third heavy-hole (dash-dotted) subbands. The notation $nCi-Hj$ ($nCi-Lj$) is explained in the text.

current spectra (Fig. 2) and their assignment to specific transitions is plotted in detail in Figs. 3(a) and 3(b), respectively. Around -14 V, both the light-hole $L1$ and the second heavy-hole $H2$ replica show the anticrossing between the $0C1$ and $-1C2$ levels in a way similar to the lowest heavy-hole $H1$ one. Consequently, the localized valence subbands act as independent probes for the delocalization of the electron states. This is an additional proof for the fact that the anticrossing is caused by the quantum states of the conduction band. The spatially direct $0C2-H1$ and $0C1-H2$ transitions could not be detected at low electric fields due to the parity selection rules.¹⁵ The anticrossing between $0C2-H1$ and $1C1-H1$, as apparent from the data in Fig. 3, shows a stronger repulsion than the one between $-1C2-H1$ and $0C1-H1$. This observation cannot be explained by the structure of the conduction band alone which would predict equally strong repulsion [see Fig. 1(a)]. Although this effect is not yet completely understood, we believe that it is due to differences in the excitonic binding energies of the respective transitions. In addition, these binding energies are sensitive to the field-dependent changes of the localization length.¹⁶ In Fig. 3(a), the structures at about 15 meV above the spatially direct $0C1-H1$ and $0C1-L1$ energies are associated with excited states of these excitonic transitions.^{16,17} They could not be resolved beyond -10 V.

Comparing Fig. 3 with Fig. 1(d), we see that the $m=1$ anticrossing gives rise to nearly identical patterns, whereas the $m=2$ resonance is not yet resolved. For reasons which are not important in the present context, higher-order (i.e., $|n| > 1$) transitions are more easily detected in $I-V$ measurements at constant wavelengths than in photocurrent spectra at constant voltages. Figure 4 shows a series of $I-V$ curves where the $-2C2-H1$ transition is well resolved. There is a clear anticrossing between $-2C2-H1$ and $0C1-H1$ (inset of Fig. 4) as ex-

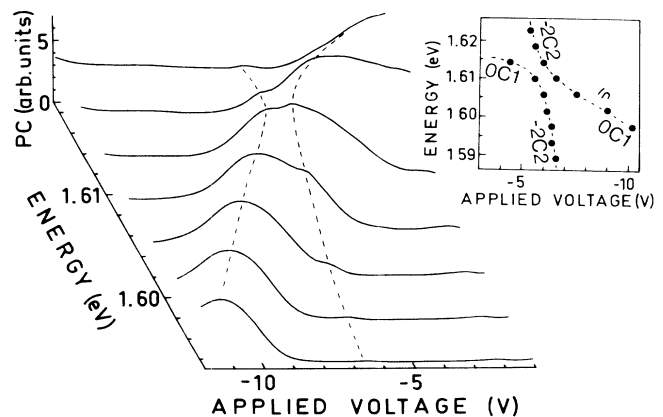


FIG. 4. $I-V$ curves at 5 K (monochromatic illumination at different energies) showing the anticrossing between the $0C1-H1$ and $-2C2-H1$ transitions. Inset: Voltage dependence of the peak energies. The dashed lines are guides for the eye.

pected from Fig. 1. We also found some weak structure associated with the $-3C2-H1$ transition. These experimental and theoretical results indicate that resonance-induced delocalization can still be observed for a large separation index m . The only practical restriction is that the resonance splitting must be larger than the linewidth of the participating excitonic transitions. The actual limit might also depend on an additional, incoherent energy broadening of the delocalized states due to the imperfections of the SL.

Finally, we note that the appearance of the $m=2$ resonance indicates the general feature that resonant interaction between different Stark ladders can already occur at low electric fields. We also performed tight-binding-like calculations which imply that the resulting delocalization can even be *stronger* than Wannier-Stark localization and prevail over the field-induced localization effects. This occurs if the (mini)bandwidth W is significantly larger than the (mini)bandgap G . In particular, this general condition is satisfied for the case of the crystal lattice of a bulk semiconductor where the bandwidth of the conduction band is at least 3 times as large as the bandgap ($W/G \geq 3$). Therefore, field-induced localization phenomena are not to be expected in bulk materials.

In conclusion, we have reported the first observation of electric-field-induced delocalization of carrier states in a SL due to resonant interaction between different Stark ladders. This effect strongly influences the optical properties of the GaAs-AlAs SL under study since the resonance splitting significantly exceeds the excitonic linewidths. We have also found that this delocalization is not only restricted to *adjacent* SL cells but is also observed between states localized in *non-neighboring* wells of the SL. Consequently, this effect provides a method to probe high-field coherence properties of electrons in SL structures.

The authors are grateful to A. Fischer for sample growth and to J. Jungbauer, F. Schartner, S. Tippmann, and M. Wurster for diode processing. This work was

supported by the Bundesministerium für Forschung und Technologie.

Note added.— More recently, we have also detected the $m=3$ resonance. Both the $m=1$ and the $m=2$ resonance are still observed at room temperature.

^(a)Present address: Fraunhofer-Institut für Angewandte Festkörperphysik, Tullastrasse 72, D-7800 Freiburg, Federal Republic of Germany.

¹J. Bleuse, G. Bastard, and P. Voisin, Phys. Rev. Lett. **60**, 220 (1988).

²E. E. Mendez, F. Agulló-Rueda, and J. M. Hong, Phys. Rev. Lett. **60**, 2426 (1988).

³P. Voisin *et al.*, Phys. Rev. Lett. **61**, 1639 (1988).

⁴G. H. Wannier, *Elements of Solid State Theory* (Cambridge Univ. Press, London, 1959), pp. 190–193; Phys. Rev. **117**, 432 (1959).

⁵J. Leo and A. MacKinnon, J. Phys. Condens. Matter **1**, 1449 (1989), and references therein.

⁶C. Zener, Proc. Roy. Soc. London A **142**, 523 (1934).

⁷G. Bastard, Phys. Rev. B **25**, 7584 (1982).

⁸H. Schneider, K. v. Klitzing, and K. Ploog, Superlattices Microstruct. **5**, 383 (1989).

⁹G. Danan, B. Etienne, F. Mollot, and R. Planel, Phys. Rev. B **35**, 6207 (1987).

¹⁰The transition from resonantly split, discrete-well states into a SL miniband was studied via absorption spectroscopy by R. Dingle, A. C. Gossard, and W. Wiegmann, Phys. Rev. Lett. **34**, 1327 (1975).

¹¹D. A. B. Miller *et al.*, Phys. Rev. Lett. **53**, 2173 (1984).

¹²H. T. Grahn, H. Schneider, and K. v. Klitzing, Appl. Phys. Lett. **54**, 1757 (1989).

¹³G. Livescu *et al.*, Phys. Rev. Lett. **63**, 438 (1989).

¹⁴H. Schneider, K. v. Klitzing, and K. Ploog, Europhys. Lett. **8**, 575 (1989).

¹⁵P. W. Yu *et al.*, Phys. Rev. B **40**, 3151 (1989).

¹⁶F. Agulló-Rueda, E. E. Mendez, J. A. Brum, and J. M. Hong, Surf. Sci. **228**, 80 (1990).

¹⁷J. J. Song *et al.*, Phys. Rev. B **39**, 5562 (1989).